Available online at www.sciencedirect.com
SCIENCE DIRECT®
Biosensors and Bioelectronics 18 (2003) 1399–1406
BIOSENSORS & BIOELECTRONICS
www.elsevier.com/locate/bios

Sensitivity of the acoustic waveguide biosensor to protein binding as a function of the waveguide properties

E. Gizeli [a,*], F. Bender [a], A. Rasmusson [a], K. Saha [a], F. Josse [b], R. Cernosek [c]

[a] Institute of Biotechnology, University of Cambridge, Tennis Court Road, Cambridge CB2 1QT, UK
[b] Microsensors Research Laboratory and Department of Electrical and Computer Engineering, Marquette University, P.O. Box 1881, Milwaukee, WI 53201-1881, USA
[c] Sandia National Laboratories, Microsensor Research and Development Department P.O. Box 5800, MS 1425, Albuquerque, NM 87185-1425, USA

Received 4 April 2002; received in revised form 27 August 2002; accepted 21 January 2003

Abstract

The aim of this work is to study the effect of operating frequency, piezoelectric substrate and waveguide layer thickness on the sensitivity of the acoustic waveguide sensor during the specific binding of an antibody by a protein. Shear horizontal (SH) wave devices consisting of (a) a $LiTaO_3$ substrate operating at 104 MHz, (b) a quartz substrate operating at 108 MHz and (c) a quartz substrate operating at 155 MHz were coated with a photoresist polymer layer in order to produce acoustic waveguide devices supporting a Love wave. The effect of the thickness of the polymer layer on the Love wave was assessed by measuring the amplitude and phase of the wave before and after coating. The sensitivity of the above three biosensors was compared during the detection of the specific binding of different concentrations of Immunoglobulin G in the range of 0.7–667 nM to a protein A modified surface. Results indicate that the thickness of the polymer guiding layer is critical for obtaining the maximum sensitivity for a given geometry but a trade-off has to be made between the theoretically determined optimum thickness for waveguiding and the device insertion loss. It was also found that increasing the frequency of operation results in a further increase in the device sensitivity to protein detection.

Keywords: Acoustic waveguide device; Love wave; Biosensor

1. Introduction

During the last few years, acoustic wave biosensors have received increasing attention and shown to be an attractive alternative to surface plasmon resonance (Gizeli and Lowe, 2002). Of the acoustic wave systems available, the low frequency (5–15 MHz) thickness shear mode (TSM) resonator has been the most popular device so far (Collings and Caruso, 1997; Cavic et al., 1999; Janshoff et al., 2000). This is mainly because TSM resonators are readily available, require a simple instrumentation and exhibit a good signal to noise ratio. Surface acoustic wave (SAW) devices, operating in the upper MHz range, i.e. from 100 to 500 MHz, exhibit a sensitivity that is several orders of magnitude higher than that of the TSM resonator since sensitivity increases with the operating frequency. The higher sensitivity of the SAW sensors has been clearly demonstrated for gas applications (Ballantine et al., 1997). However, their application in liquid sensing is still limited, mainly because the shear horizontal (SH) SAW devices required for liquid sensing are not yet readily available.

Of the available SH-SAW devices, the Love wave device has been shown to be the most promising platform for sensing applications (Gizeli et al., 1992; Kovacs and Venema, 1992). This sensor platform comprises a waveguide geometry where a shear-operating SAW device is overlayed by a layer of a dielectric material (Fig. 1). The main advantage of the waveguide device is that the acoustic energy is confined to the sensing surface resulting in higher sensitivity to surface perturbations. Waveguides consisting of a single layer of

* Corresponding author. Tel.: +44-1223-334160; fax: +44-1223-334162.
E-mail address: e.gizeli@biotech.cam.ac.uk (E. Gizeli).

0956-5663/03/$ - see front matter
doi:10.1016/S0956-5663(03)00080-0

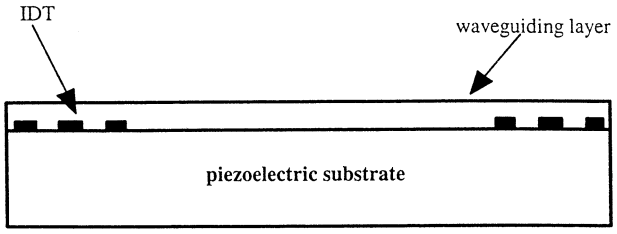

Fig. 1. Schematic representation of the acoustic waveguide geometry: the piezoelectric substrate supports SH waves which are excited and detected by using a pair of IDTs. The entire surface of the piezoelectric substrate including the IDTs is coated with a waveguiding layer (Novolac).

silica (Du et al., 1997; Freudenberg et al., 2001), polymethylmethacrylate (PMMA) (Gizeli, 1997; Bender et al., 2000) and photoresist (Rasmusson and Gizeli, 2001; McHale et al., 2001), or a multilayer of silica and PMMA (Du and Harding, 1998) have been reported. In general, polymer waveguides are desirable since they can be easily constructed by using spin coating method instead of the laborious procedures required for silica deposition. Acoustic waveguide devices employing polymer and silica layers have been used in biosensing applications to detect antibody-antigen (Gizeli et al., 1997; Harding et al., 1997; Bender et al., 2000) and antibody-peptides (Gizeli et al., 1996) interactions as well as the formation of supported lipid bilayers (Melzak et al., 2001).

In order to use the acoustic waveguide device for biosensing experiments it is important to optimise the acoustic geometry. One of the parameters that has been extensively studied is the effect of the waveguide thickness on the device sensitivity; these studies involve the utilisation of both various SH-wave devices and biological molecules. Since the sensitivity of biosensors depends on both the transducer and biological molecule used, it is important to compare different acoustic wave devices for the detection of the same biological interaction. For this reason, in this study the performance of three acoustic waveguide biosensors during the detection of the same biological recognition event are being compared as a function of operating frequency, piezoelectric substrate and waveguide layer thickness. Two quartz devices operating at 108 MHz (Q108) and 155 MHz (Q155) and one lithium tantalate (LT) device operating at 104 MHz (LT104) were used as the substrate in a waveguide configuration employing a photoresist, Novolac, as the waveguiding layer. Novolac, a formaldehyde/phenyl commercially available photoresist, was chosen among other polymers due to its good chemical stability (Rasmusson and Gizeli, 2001). The effect of the thickness of Novolac on the device performance was studied by monitoring the frequency and insertion loss of each device before and after deposition. Finally, the sensitivity of each waveguide biosensor was compared during the binding of different concentrations of Immunoglobulin G (IgG) to surface-bound protein A.

2. Experimental section

2.1. Materials

Phosphate buffered saline tablets, pH 7.4 (0.01 M phosphate, 2.7 mM potassium chloride and 0.137 M sodium chloride), 2-ethoxy-ethyl acetate and protein A were purchased from Sigma. Novolac photoresist was purchased from Shipley. Monoclonal IgG, raised against the hormone estrone 3 glucaronide (anti-E3G IgG), was obtained from Unilever Research, Colworth, UK.

2.2. Devices

2.2.1. Q108 MHz

The 108 MHz quartz device was fabricated on a 0.5 mm thick piezoelectric quartz crystal, specifically a rotated Y-cut (42.5°) quartz with propagation 90° with respect to the x-axis. The interdigital transducer (IDTs) comprised of 10/200-nm thick chromium/gold electrode and consisted of 80 pairs of split fingers with a periodicity of 45 μm.

2.2.2. Q155 MHz

The 155 MHz quartz device was fabricated on a 0.5-mm thick crystal and comprised of 92 electrode pairs. The devices are fabricated with 120-nm-thick Cr/Au (20/100 nm) split finger IDTs having a period of 32 μm. The device utilized a dual delay line configuration where one delay line could act as the reference line and the other as the sensing line.

2.2.3. LT104 MHz

The LT device was fabricated on a 0.5-mm thick rotated Y-cut (36°), X-propagating crystal with 90-nm-thick, and 28 pairs of Cr/Au (20/70 nm) split finger IDTs having a period of 40 μm. A dual delay line configuration was also used. Using a dual delay line configuration with one line as the reference line and the other as the sensing line makes temperature control essentially unnecessary.

A schematic representation of each device is shown in Fig. 2.

2.3. Instrumentation

For the Q108 MHz device a Hewlett-Packard 4195A Network Analyser was used to monitor the frequency and phase of the wave together with an HPVEE program. To minimise interfering reflections the device was

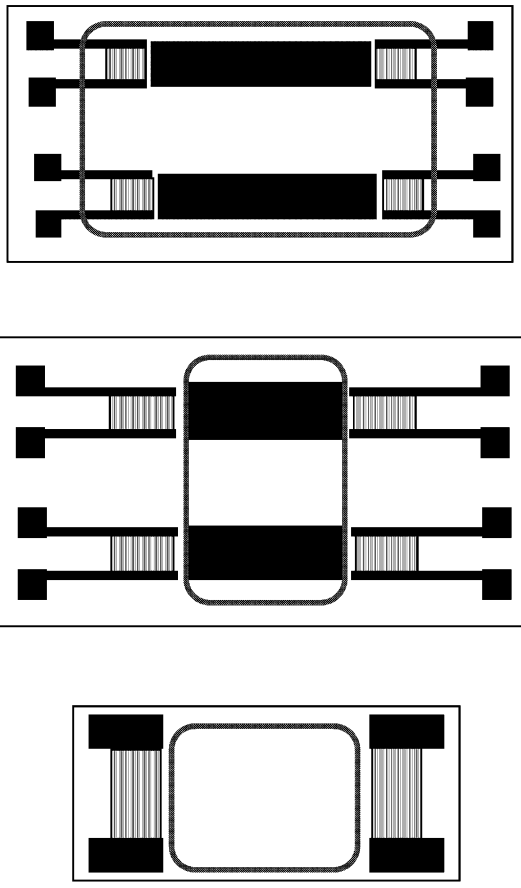

Fig. 2. Schematic representation of the three acoustic waveguide devices, i.e., the LT104, Q155 and Q108. Note that the surface between the first two include a metallised layer between the IDTs; also in the case of LT 104, the IDTs are exposed to liquid.

measured with scotch tape on the back. For the Q155 and LT104, a Hewlett-Packard 8753ES Network Analyser was used for performing the measurements together with a VEE software programme for collecting data. The Fourier transform/time gating function of the device was used for the biosensing measurements in order to minimise unwanted interference with electromagnetic feed-through and triple transit signals.

2.4. Novolac deposition

Different polymer concentrations were prepared by diluting the polymer in 2-ethoxy-ethyl acetate. Novolac solutions (10, 20, 30, 40, 50, 60, 70, 80% w/w) were applied on the device surface by using a spin coater (Speciality Coating Systems P6700) at 4000 rpm for 40 s. The solvent was evaporated by heating the coated device in an oven at 190 °C for 2 h. The devices were measured before and after coating with the polymer and the frequency and amplitude changes were recorded. The thickness of the waveguide layer was measured by using a surface profilometer (Dektak).

2.5. Device cleaning

The Novolak coated Q108 MHz devices were cleaned by soaking them in 4 M sodium hydroxide for at least 1 h and then placing them in a sonicating bath for 20 min in sodium hydroxide followed by distilled water rinse. The Q155 and LT104 Novolak coated devices were treated with sodium hydroxide solution as above and then were dipped into freshly prepared and still hot (50 °C) piranha solution, consisting of sulphuric acid (97%) and hydrogen peroxide (27.5%) in a ratio of 3:1 (v/v), for 5 min.

2.6. Gold deposition

The area between the IDTs on the Novolak device was coated with 10 nm of gold by thermal evaporation at a pressure of less than 5.0×10^{-6} mbar using an Edwards (Auto 306) evaporator.

2.7. Liquid-based experiments

Each device was mounted in a special holder and the liquid was pumped through using a peristaltic pump and a flow through cell. The flow cell was sealed on the surface by using a custom-made rubber gasket. Due to the different size of each device, three different flow cells were manufactured exposing 0.12, 0.12 and 0.06 cm^2 of the LT104, Q108 and Q155 devices, respectively, to the solution. A schematic representation of the different sensing areas is shown in Fig. 2.

2.8. Protein A-IgG binding

The freshly prepared gold-surface was placed in the device holder and exposed to PBS buffer for approximately 1 h and at a flow rate of 83 μl/min. Protein A in a concentration of 50 μg/ml in PBS was added and left in contact with the device surface at the above flow rate for 30 min. Different solutions of monoclonal antibodies of anti-E3G at a concentration range of 0.7–667 nM in PBS were finally added to the device surface followed by buffer rinse.

3. Results

The transmission spectrum of each device was monitored by using a Network Analyser before and after depositing a Novolac layer. For initial device characterisation, the Fourier transform/time gating function was turned off so all features including signal interferences and distortions could be evaluated. The deposition of a polymer layer changed the wave amplitude (A) and transmitted frequency (f). Fig. 3 shows the transmission spectrum of the Q155 and LT104 devices before and

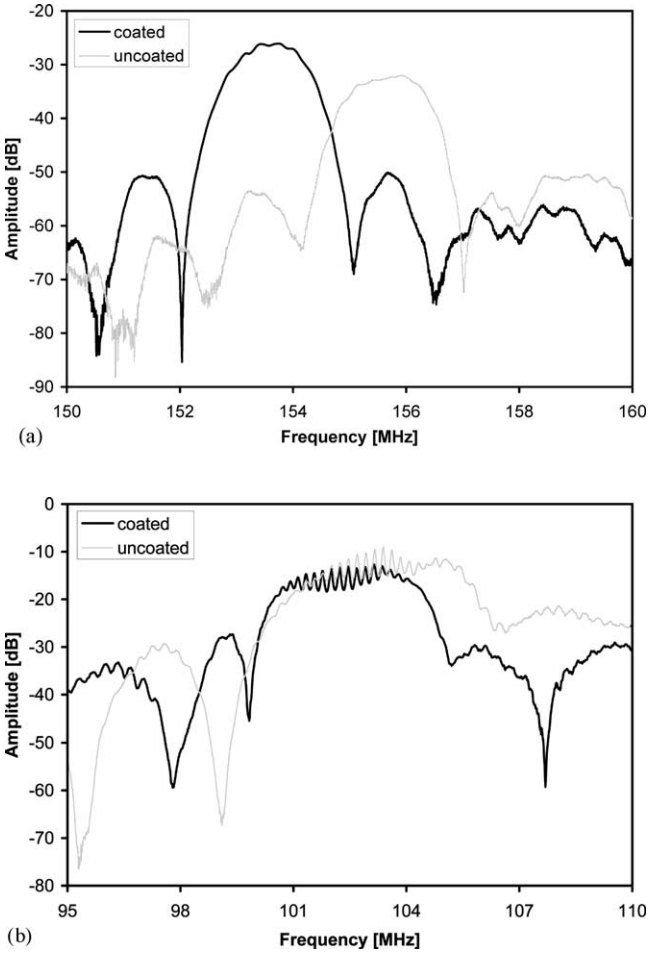

Fig. 3. (a) Transmission spectrum of the quartz 155 MHz (Q155) device where amplitude is plotted as a function of frequency before and after the device is coated with 0.87 μm of Novolac; (b) transmission spectrum of the $LiTO_3$ 104 MHz (LT104) device where amplitude is plotted as a function of frequency before and after the device is coated with 1.75 μm of Novolac.

after coating them with a polymer layer of Novolac of 0.87 and 1.75 μm, respectively. The ripples visible on the main transmission passband of the LT104 device (Fig. 3b) are due mainly to acoustic reflections from the IDT fingers (triple transit echo) caused by the high piezoelectric coupling constant of $LiTaO_3$. When immersed in liquid and/or covered with a bioreceptive layer, the device will show a smaller ripple due to the added attenuation in the system. Another consequence of the high $LiTaO_3$ coupling constant is the smaller number of required electrode finger pairs compared to the quartz devices, resulting in a broader frequency transmission peak.

Fig. 4(a) and (b) show the measured frequency (Δf) and amplitude (ΔA) change, respectively, as a function of the normalised Novolac thickness. Frequency and amplitude changes are defined as the frequency and amplitude of the coated Love wave device minus that of the uncoated device. The normalised thickness is defined as the ratio of the measured thickness (h) divided by the acoustic wavelength in the guiding layer (λ_{Nov}). The latter is related to the operating frequency (f_o) through: $\lambda = v_{Nov}/f_o$, where f_o is 108, 155 and 104 MHz for the Q108, Q155 and LT104 devices, respectively, and v_{Nov} is 1100 m/s.

The sensitivity of the three different waveguide devices was studied during the specific binding of a protein on the device surface. The surface of all three waveguide devices was prepared and treated in the same manner in order to minimise any differences in antibody binding due to variations in the surface morphology. Protein A, which is known to have a strong affinity for gold, was adsorbed on the freshly prepared gold surface (data not shown) and used, subsequently, for binding different concentrations of IgG. The device phase was found to be significantly more sensitive than the amplitude and for this reason was monitored preferentially during antibody binding. Fig. 5 shows the phase response of the three devices during the binding of different concentrations of IgG to the protein A activated surface. Due to the different areas exposed to the protein solutions, phase change was expressed as a function of the sensing area for each device. Note that the corresponding frequency changes can be easily obtained from the measured phase changes.

4. Discussion

4.1. Waveguide geometry

When the surface of a SH-SAW devices is covered with an overlayer of a dielectric material which has a lower shear acoustic velocity (v_o) than the piezoelectric substrate (v_s), then the SH-SAW is converted to a guided wave known as the Love wave. For a specific frequency, the velocity of the Love wave (v_L) depends on the thickness of the overlayer and can vary between v_o and v_s, i.e. $v_o < v_L < v_s$. In this work the photoresist Novolac is applied as a waveguide layer on the surface of three devices. The effect of the thickness of the layer on the frequency and, thus, propagating velocity of the Love wave is shown in Fig. 4(a). When thin overlayers are applied, the velocity of the guided wave is close to that of the substrate and the frequency change is small; as the overlayer thickness increases the velocity decreases until eventually it will reach the velocity of Novolac, resulting in a larger frequency drop. Fig. 4(a) shows that, for a given overlay material, the frequency change of the Love wave depends on the piezoelectric material used for the acoustic device. The larger rate of frequency change observed with the two quartz devices is due to the larger difference between the acoustic shear velocities in quartz ($v_Q = 5000$ m/s) and Novolac ($v_{Nov} = 1100$ m/s) than in LT ($v_{LT} = 4120$ m/s) and Novolac.

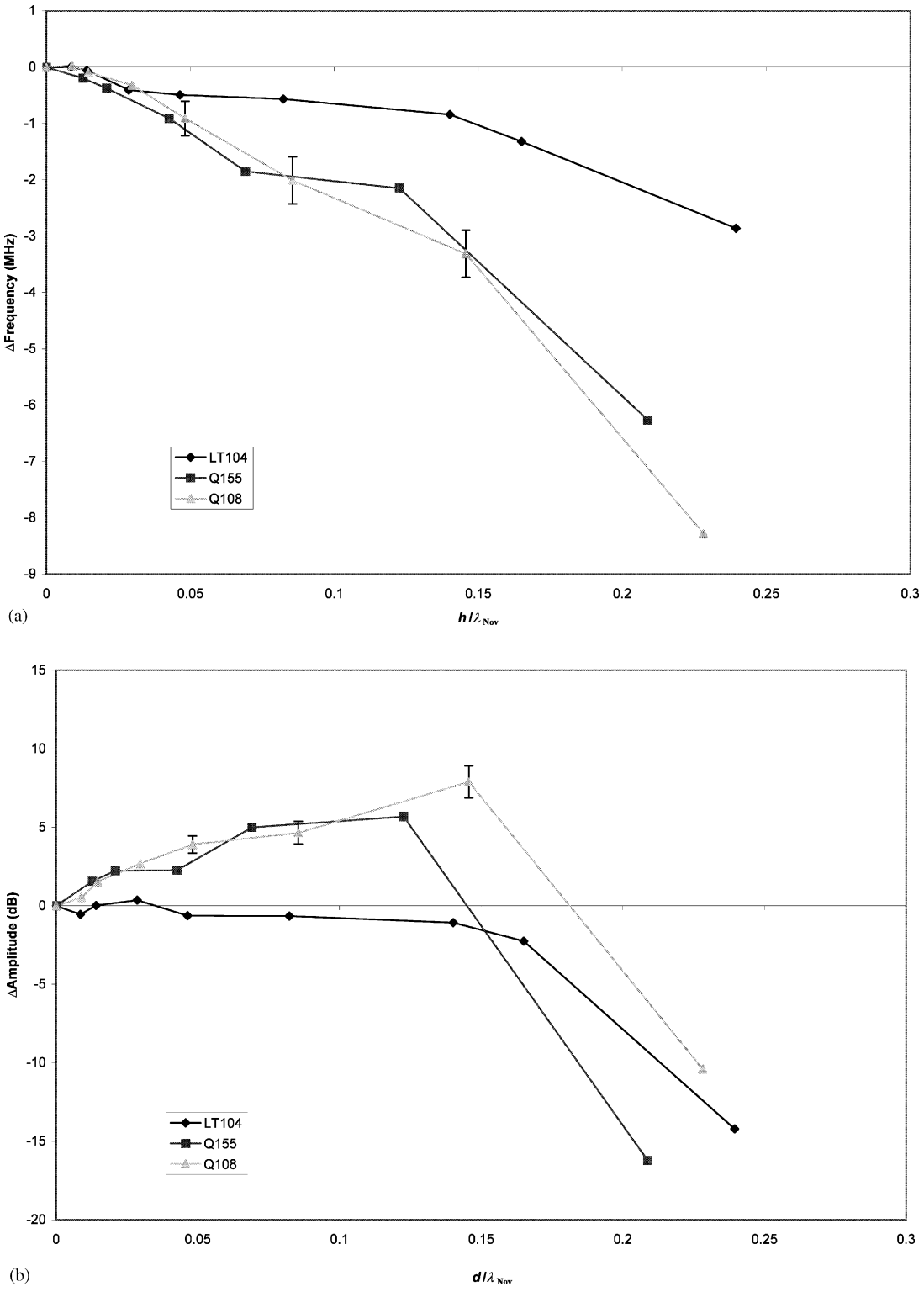

Fig. 4. (a) Frequency and (b) amplitude change as a function of the normalised thickness (h/λ_{Nov}), where h is the Novolac thickness and λ_{Nov} the acoustic wavelength inside the layer for the $LiTO_3$ 104 MHz (LT104), quartz 155 MHz (Q155) and quartz 108 MHz (Q108) devices.

The effect of the overlayer thickness on the transmitted RF power of the acoustic wave is shown in Fig. 4(b). The positive amplitude change observed with the quartz substrate indicates that more acoustic energy is trapped close to the upper surface of the device as the thickness of Novolac increases until a critical normalised thickness is reached, which was 0.15 ($h = 1.5$ μm) and 0.12 ($h = 0.9$ μm) for the Q108 and Q155 devices,

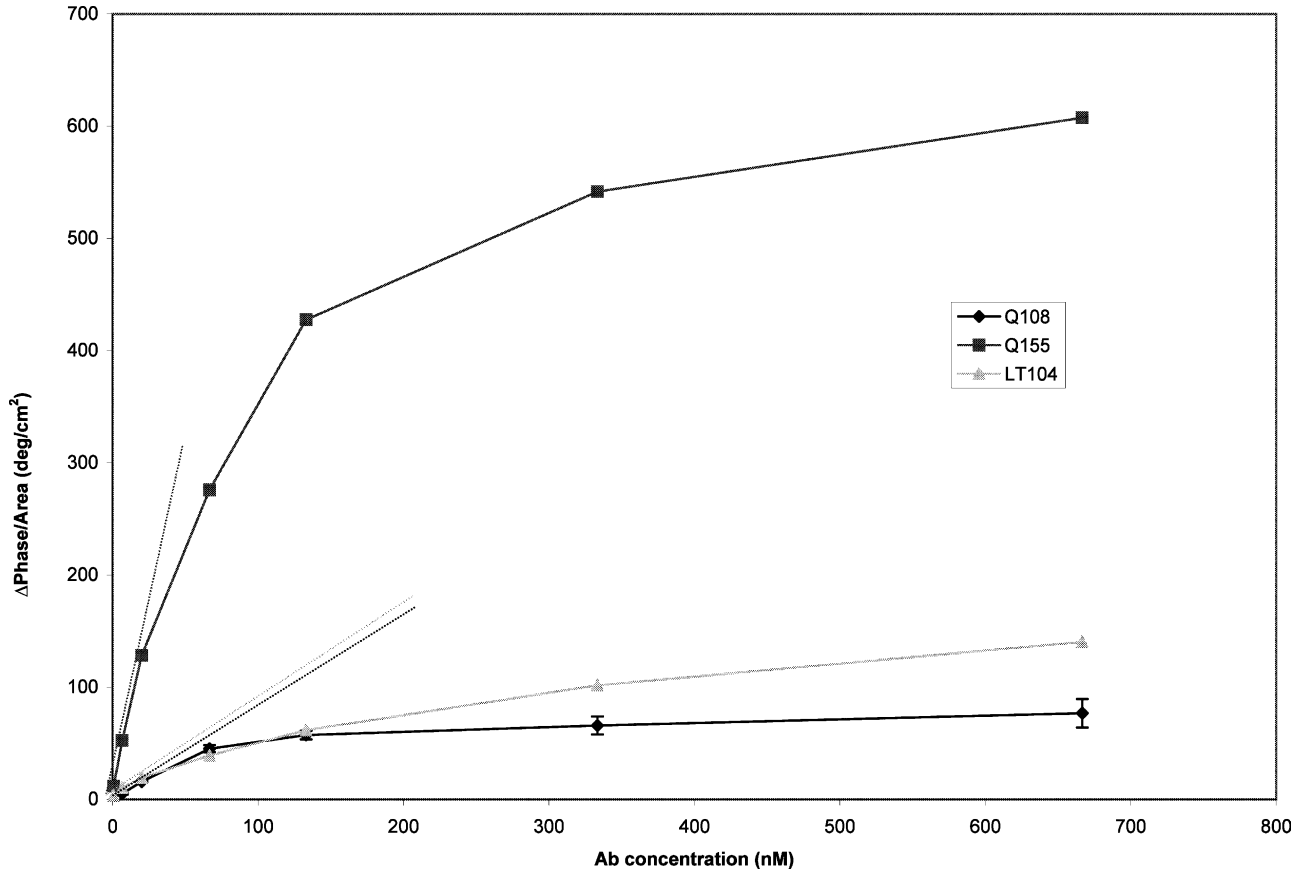

Fig. 5. Phase change as a function of the sensing area during IgG binding to the protein A modified surface of the $LiTO_3$ 104 MHz (LT104), quartz 155 MHz (Q155) and quartz 108 MHz (Q108) devices.

respectively. This behaviour is characteristic of the nature of the SH waves that travel inside the uncoated quartz substrate; this wave, known as the surface skimming bulk wave, diffracts into the bulk of the crystal resulting in high energy loss (Browning and Lewis, 1997). The effect of the waveguide layer is to trap more energy on the device surface and increase the acoustic efficiency of the SH-wave transmission on the device surface. For higher Novolac thicknesses the signal becomes very lossy, possibly because the Love wave is guided predominantly inside Novolac, which is acoustically very lossy compared to the piezoelectric substrate materials. Fig. 4(b) shows that the efficiency of the guiding of the Love wave in the Novolac/LT device follows a different pattern. The conversion of the SH wave to a guided Love wave does not have a significant effect on the efficiency of the transmission for normalised thicknesses up to 0.14 ($h = 1.5$ μm). This is because the metallised $LiTaO_3$ used for this work supports predominantly a SH-SAW, which, due to the large piezoelectric coefficient of $LiTaO_3$, is already guided near the surface and does not diffract into the bulk of the crystal. For normalised thicknesses above 0.14 the signal becomes again significantly more lossier. Apparently, above that thickness the wave is located predominantly inside the Novolac layer and the device exhibits the same high-loss observed with the quartz substrate. From the above it can be concluded that the cut-off critical normalised thickness $(h/\lambda_{Nov})^{crit}$ is a characteristic of the properties of the waveguide material and does not depend on the device operating frequency or piezoelectric substrate.

For biosensing experiments, it is highly desirable to use the most sensitive waveguide geometry for each device. Fig. 4(a) can be used as a guide for choosing the Novolac thickness that gives the highest sensitivity, i.e. the region of the graph where the rate of frequency change with thickness change is the largest. However, for the Q108 waveguide biosensor, calibration of the mass sensitivity as a function of the polymer thickness showed that the insertion loss of the device was the most critical parameter for choosing the optimum guiding layer thickness (Gizeli, 1997). For this reason, normalised thickness of Novolac layer of 0.15 and 0.12 for the Q108 and Q155 device, respectively, was used for the biosensing experiments. The normalised Novolac thickness of the LT104 was chosen to be 0.14, based on previous experimental data (Bender et al., 2000).

4.2. Sensitivity to protein binding

Fig. 5 shows the phase change of the devices during the binding of IgG to the protein A modified surface as a function of the IgG concentration. If the phase change is assumed to be directly proportional to the surface density of the IgG, then Fig. 5 can be described by using the Langmuir isotherm model (Andrade, 1985). Based on this model and for low IgG concentrations, the phase changes linearly with [IgG] while at higher concentrations the phase response saturates as a result of the saturation of protein A binding sites. Given the above, the first part of the $\Delta\phi$ versus [IgG] graph can be used to experimentally determine the sensitivity of each device to mass deposition during protein binding.

The mass sensitivity (S_m) of acoustic wave sensors is defined as the relative change in the frequency due to mass loading divided by the surface density of the deposited mass:

$$S_m = \lim_{m\to 0}\left[\frac{\frac{\Delta f}{f_o}}{\frac{\Delta m}{A}}\right] \quad (1)$$

where Δf is the frequency change, f_o the operating frequency and $\Delta m/A$ the deposited mass per unit area. In this experimental set-up, phase change is measured and is related to frequency through the following relationship:

$$\frac{\Delta f}{f_o} = \frac{\Delta\phi\lambda_s}{360L} \quad (2)$$

where ϕ is the wave phase in degrees, λ_s is the acoustic wavelength in the substrate and L is the length of the propagation path of the wave. Based on Eq. (2) and on the assumption that for low concentrations the antibody mass deposition is proportional to bulk antibody concentration, Eq. (1) becomes:

$$S_m = \lim_{[IgG]\to 0}\left[\frac{\frac{\Delta\phi\lambda_s}{360L}}{\frac{\Delta C[IgG]}{A}}\right] \quad (3)$$

where [IgG] is the bulk antibody concentration in solution and C is an arbitrary constant proportional to the bulk concentration of IgG. Eq. (3) can be further simplified and rewritten as:

$$S_m = \frac{\lambda_s A}{360LC}\lim_{[IgG]\to 0}\left[\frac{\Delta\phi}{\Delta[IgG]}\right] \quad (4)$$

By estimating the slope of $\Delta\phi$ versus [IgG] based on Fig. 5 and by inserting the corresponding data from Table 1 into Eq. (4), the following ratio of sensitivities are obtained: $S_m^{Q155}/S_m^{Q108} = 1.3$ and $S_m^{Q108}/S_m^{LT104} = 1.1$.

Table 1
Data used for calculating mass sensitivity S_m

Parameter	Q155	Q108	LT104
$\lim_{[IgG]\to 0}(\Delta\phi/\Delta[IgG])$[a] (°/nM)	0.359	0.095	0.096
λ_{sub} (μm)	32	45	40
L (μm)	9400	9000	9000
A (cm^2)	0.06	0.12	0.12

[a] Estimated from slope of linear regression fit for $\Delta\phi$ versus [IgG] plot based on Fig. 5.

The similar mass sensitivity measured with the $LiTaO_3$ and quartz devices was not surprising since both devices operate at a similar frequency. From theoretical considerations one would expect that for the same frequency the mass sensitivity of the quartz-based waveguide sensor would be higher than for $LiTaO_3$ due to the higher SH-SAW velocity in quartz. However, the $LiTaO_3$ devices used for this work were completely immersed in liquid during the experiments, including the coated IDTs because $LiTaO_3$ exhibits dielectric constant about an order of magnitude higher than that of quartz. This means that even in contact with a liquid of a high dielectric constant like water, efficient piezoelectric transduction can still take place in the IDTs while the insertion loss can still remain as low as 24 dB. In the case of the quartz devices, only the propagation path between the IDTs could be immersed in liquid and exposed to the analyte, and even that resulted in a device with a high insertion loss (40 dB) and possibly a proportionate reduction in sensitivity. The remaining difference in sensitivity for the two materials is predicted to be small. It is worth mentioning that the higher phase change observed with LT104 at high IgG concentrations is probably due to the non-specific binding of IgG on the Novolac surface which is also in contact with the antibody solution.

For a given mass density deposited on the surface, mass sensitivity defined in Eq. (1) is expected to increase with the operating frequency (Ballantine et al., 1997). Thus, the ratio in the sensitivities of the Q155 to Q108 devices should be 1.43, i.e. slightly larger than what was experimentally measured. The reason for this discrepancy is most likely due to the different normalised Novolac thickness used in each waveguide; i.e. 0.12 and 0.15 for the Q155 and Q108 devices, respectively, which would result in different amounts of the acoustic wave being localised in the waveguide.

It is worth mentioning that the acoustoelectric interaction during antibody binding should be taken into account for the Q108 device, as the sensing surface is not electrically shorted in contrast to the Q155 and LT104 devices. The elastic behaviour of the polymer waveguides will also slightly depend on frequency and can have an effect on the device performance. Finally, bound IgG was treated as being purely elastic and the

viscoelastic nature of the antibody layer was not taken into account.

5. Conclusions

The normalised thickness ($h/\lambda_{Polymer}$) of the polymer layer appears to be a critical parameter in designing sensitive acoustic waveguide biosensors. It was shown that the maximum mass sensitivity would occur for an overlayer thickness equal to $h = (\lambda_{Nov}/4)$ (McHale et al., 2002). Since the insertion loss of the composite device is the only reason for keeping $h/\lambda_{Polymer}$ lower than 0.25, the materials consideration of attenuation in the polymer waveguide is the limiting factor in the sensitivity of a device. Future optimisation work should include attempts to find waveguide materials that allow devices to operate closer to the theoretically predicted quarter wavelength criterion. Waveguide materials with a low shear velocity and low insertion loss seem to be the most promising materials for developing sensitive biosensors.

From the above considerations, it is evident that a further increase in frequency of operation will result in a large increase in mass sensitivity of the acoustic waveguide sensors. This is not surprising since at higher frequency, the wave is naturally guided closer to the surface. As a result, a thinner layer is also needed for further optimisation for higher sensitivity. On the other hand, sensitivity considerations will not result in a clear preference for one of the two materials used. But besides mass sensitivity, this choice will be influenced by other device characteristics as well. Due to the large differences in their piezoelectric constants, the transmission characteristics of guided SH-SAWs on quartz and $LiTaO_3$ exhibit some pronounced differences as evident in Fig. 3. Even though the deposition of a waveguide results in an increase in overall loss in case of the LT104 device, the resulting loss is still significantly smaller than for the quartz devices. This is due not only to the smaller piezoelectric constants of quartz, but also to the fact that for the quartz devices, a flow cell has to be placed between the IDTs as discussed above. The rubber gasket of the cell pressed onto the device surface will slightly disturb the acoustic wave, resulting in an increase in overall loss. However, if the device is incorporated into an oscillator circuit, the total loss of the device must not exceed the gain of the amplifier in order to maintain oscillation. Thus, in this situation, the low-loss design of the LT104 device offers important advantages.

The major drawback of the high piezoelectric constants of $LiTaO_3$ is the triple transit echo evident in Fig. 3(b). If lossy films are deposited onto the device, and/or if the device is operated in a liquid environment exhibiting high viscoelastic loss, the ripple simply disappears because the triple transit echo will experience three times the loss experienced by the main wave. Thus, it appears that in high-loss applications, $LiTaO_3$ seems to be the substrate material of choice while in low-loss applications quartz may exhibit better wave characteristics.

Acknowledgements

Dr E. Gizeli would like to acknowledge Dr M. Newton and Dr McHale for helpful discussions and technical assistance, Unilever for donating the antibody used in this work and BBSRC for supporting financially this work. Prof. F. Josse would like to acknowledge the financial support of the National Science Foundation (NSF). Dr R. Cernosek would like to acknowledge Sandia National Laboratories for supporting this work under Contract DE-AC04-94AL85000.

References

Andrade, J.D., 1985. Surface and Interfacial Aspects of Biomedical Polymers. Plenum, New York.
Ballantine, D.S., White, R.M, Martin, S.J., Ricco, A.J., Zellers, E.T, Frye, G.C., Wohltjen, H., 1997. Acoustic Wave Sensors: Theory, Design and Physicochemical Applications. Academic Press, San Diego.
Bender, F., Cernosek, R., Josse, F., 2000. Electronics Letters 36, 1672–1673.
Browning, T., Lewis, M., 1997. Electronics Letters 13, 128–130.
Cavic, B.A., Hayward, G.L., Thompson, M., 1999. Analyst 1999, 1405–1420.
Collings, A.F., Caruso, F., 1997. Reports on Progress in Physics 60, 1397–1445.
Du, J., Harding, G., 1998. Sensors and Actuators A 65, 152–159.
Du, J., Harding, G.L., Collings, A.F., Dencher, P.R., 1997. Sensors and Actuators A 60, 54–61.
Freudenberg, J., von Schickfus, M., Hunklinger, S., 2001. Sensors and Actuators B 76, 147–151.
Gizeli, E., 1997. Smart Materials and Structures 6, 700–706.
Gizeli, E., Liley, M., Lowe, C.R., Vogel, H., 1997. Analytical Chemistry 69, 4808–4813.
Gizeli, E., Lowe, C.R. (Eds.), Biomolecular Sensors. Taylor and Francis, London 2002.
Gizeli, E., Lowe, C.R., Liley, M., Vogel, H., 1996. Sensors and Actuators B-Chemical 34, 295–300.
Gizeli, E., Stevenson, A.C., Goddard, N.J., Lowe, C.R., 1992. Ieee Transactions on Ultrasonics Ferroelectrics and Frequency Control 39, 657–659.
Harding, G., Du, J., Dencher, P., Barnett, D., Howe, E., 1997. Sensors and Actuators A 61, 279–286.
Janshoff, A., Galla, H.-J., Steinem, C., 2000. Angewandte Chemie International Edition 39, 4004–4032.
Kovacs, G., Venema, A., 1992. Applied Physics Letters 61, 639–641.
McHale, G., Newton, M.I., Martin, F., 2002. Journal of Applied Physics 31, 9701–9710.
McHale, G., Newton, M.I., Martin, F., Gizeli, E., Melzak, K.A., 2001. Applied Physics Letters 79, 3542–3543.
Melzak, K., Ralph, E., Gizeli, E., 2001. Langmuir 17, 1594–1598.
Rasmusson, A., Gizeli, E., 2001. Journal of Applied Physics 90, 5911–5914.